NMR Studies of the Role of Hydrogen Bonding in the Mechanism of Triosephosphate Isomerase†

Thomas K. Harris, Chitrananda Abeygunawardana, and Albert S. Mildvan*

Department of Biological Chemistry, The Johns Hopkins University School of Medicine, Baltimore, Maryland 21205

Received August 18, 1997; Revised Manuscript Received October 8, 1997⊗

ABSTRACT: Triosephosphate isomerase (TIM) catalyzes the reversible interconversion of dihydroxyacetone phosphate (DHAP) and glyceraldehyde-3-phosphate (GAP), with Glu-165 removing the *pro-R* proton from C1 of DHAP and neutral His-95 polarizing the carbonyl group of the substrate. TIM and its complexes with the reactive intermediate analogs, phosphoglycolic acid (PGA) and phosphoglycolohydroxamic acid (PGH), were studied by ^{1}H NMR at 600 MHz and at low temperature (−4.8 °C). His-95 shows an NϵH resonance at 13.1 ppm which shifts to 13.3 ppm in the TIM−PGA complex and to 13.5 ppm in the TIM−PGH complex. In the TIM−PGH complex, His-95 NϵH shows a slow, pH-independent exchange rate with water (k_{ex} = 80 s^{-1} at 30 °C, E_{act} = 19 kcal/mol), which is 44-fold slower than that of an exposed histidine suggesting partial shielding from bulk solvent, and a fractionation factor $\phi = 0.71 \pm 0.02$ consistent with its donation of a normal hydrogen bond. The formation of the TIM−PGH complex results in the appearance of several deshielded proton resonances, including one at 14.9 ppm and one at 10.9 ppm which overlaps with another resonance. The resonance at 14.9 ppm is absent and the resonance at 10.9 ppm is much weaker in the TIM complex of PGA, which lacks the hydroxamic acid (−NHOH) moiety. ^{15}N-labeled PGH was synthesized and the NH proton of free [^{15}N]PGH shows a single ^{1}H−^{15}N HMQC cross peak with $\delta(^1H) = 10.3$ ppm and $\delta(^{15}N) = 168$ ppm which shifts to $\delta(^1H) = 10.9$ ppm and $\delta(^{15}N) = 174$ ppm in the TIM complex of [^{15}N]PGH. The ^{15}N−^{1}H coupling in the complex indicates covalent N−H bonding, and the deshielded $\delta(^{15}N)$ indicates a significant contribution of the imidate resonance form of PGH. The 14.9 ppm resonance is assigned to the NOH proton of bound PGH. This resonance shows a pH-independent exchange rate with water (k_{ex} = 3900 s^{-1} at 30 °C, E_{act} = 8.9 kcal/mol) which may reflect the dissociation of the TIM−PGH complex, and meets the criteria for a low-barrier hydrogen bond on the basis of the significant downfield shift of 6.2 ppm from the NOH proton of the model compound acetohydroxamic acid, and a very low fractionation factor $\phi = 0.38 \pm 0.06$. In the X-ray structure of the TIM−PGH complex [Davenport, R. C., Bash, P. A., Seaton, B. A., Karplus, M., Petsko, G. A., and Ringe, D. (1991) *Biochemistry 30*, 5821], the NOH proton of bound PGH is hydrogen bonded to Glu-165. A low-barrier hydrogen bond from PGH NOH to Glu-165 suggests a dual role for Glu-165 in catalysis of proton transfer not only between the C1 and C2 carbons but also between the O1 and O2 oxygens in the interconversion of DHAP and GAP in wild type TIM. Such a mechanism, together with the measured exchange rate of the His-95 NϵH proton with solvent protons can accommodate the classical measurements of tritium incorporation from DHAP into GAP.

Triosephosphate isomerase (TIM)[1] catalyzes the diffusion-controlled reversible tautomerization of dihydroxyacetone phosphate (DHAP, **1**) to glyceraldehyde-3-phosphate (GAP, **3**) with a 10^9-fold rate enhancement. Scheme 1 depicts the simplest mechanism as proposed by Knowles and co-workers (*1*−*3*). In this mechanism the reaction is initiated by proton abstraction by the general-base catalyst, Glu-165, concerted with protonation of or hydrogen bond donation to the enolate oxygen by His-95 to form the enediol(ate) intermediate (**2**). It is not known whether the imidazolate anion exists as a stable intermediate. Protonation of the intermediate at C2 by Glu-165, concerted with deprotonation of O1 generates the product. A proposed modification of this mechanism involves the formation of an unusually strong low-barrier hydrogen bond (LBHB) between the acid catalyst, His-95, and the incipient enediolate intermediate (*4*, *5*). An alternative mechanism involves the direct transfer of the C1 hydroxyl proton to the enolate oxygen at C2 in a subsequent step without the direct participation of His-95 (*6*). To distinguish among these proposed mechanisms, we have performed ^{1}H NMR experiments at 600 MHz and at low temperature (−4.8 °C) on TIM and its complexes with analogs of the enediol(ate) intermediate phosphoglycolohy-

† This research was supported by a grant from the National Institutes of Health (DK 28616). Dr. Harris was supported by a fellowship from the National Institutes of Health (GM 17514).

* To whom correspondence should be addressed.

⊗ Abstract published in *Advance ACS Abstracts,* November 15, 1997.

[1] Abbreviations: TIM, triosephosphate isomerase; DHAP, dihydroxyacetone phosphate; GAP, glyceraldehyde-3-phosphate; LBHB, low-barrier hydrogen bond; PGH, phosphoglycolohydroxamic acid; PGA, phosphoglycolic acid; Tris-d_{11}, perdeuterated tris(hydroxymethyl)-aminomethane; DMSO-d_6, perdeuterated dimethyl sulfoxide; HMQC, heteronuclear multiple quantum coherence; NOE, nuclear Overhauser effect; NOESY, nuclear Overhauser effect spectroscopy; S/N, signal to noise ratio; SS-NOESY, symmetrically shifted NOESY; TSP, 3-(trimethylsilyl)propionate-2,2,3,3-d_4; TPPI, time-proportional phase incrementation.

S0006-2960(97)02039-4 CCC: $14.00

Scheme 1

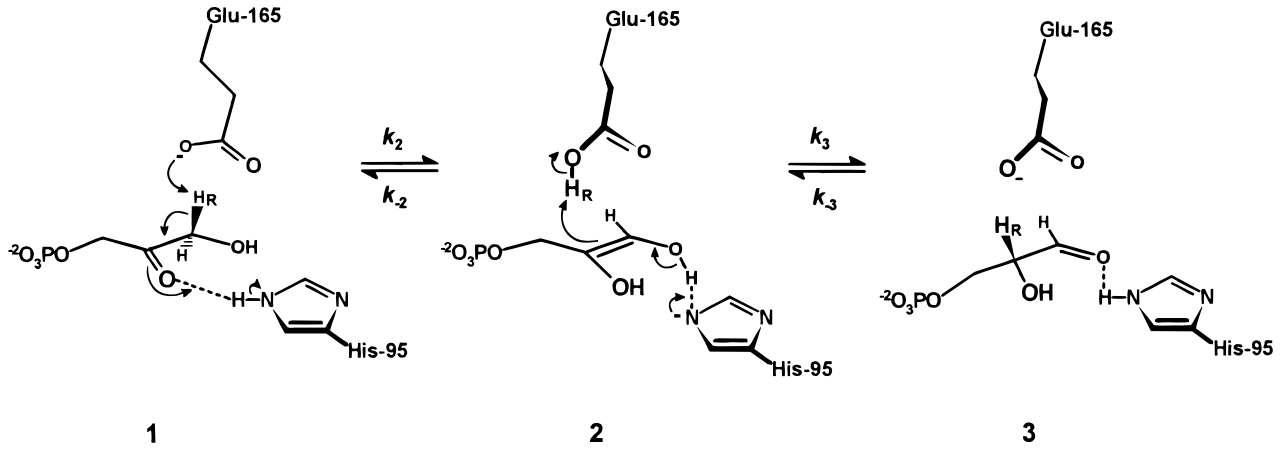

droxamic acid (PGH, **4**) (*7*) and phosphoglycolic acid (PGA, **5**) (*8*).

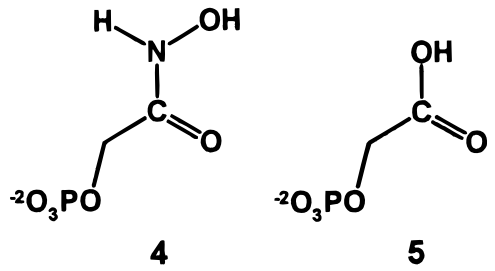

The general-base catalyzed abstraction of a proton adjacent to a carbonyl group is a common elementary step among various enzymes; however, the α-protons of carbon acids are not very acidic, and the general-base catalysts are not very basic. This presents a large thermodynamic barrier and the source of enzymatic rate enhancement for these reactions has long been a matter of discussion. Albery and Knowles (*2*, *3*) proposed that enzyme-catalyzed rate enhancement is achieved in part by reducing the thermodynamic barrier (ΔG°) of those elementary steps the transition states of which are kinetically significant, and in part by lowering their kinetic barrier. These effects were assumed to be achieved by the concerted deprotonation of C1 and protonation of the C2 carbonyl oxygen (Scheme 1). As a result, the TIM complexes with **1**, **2**, and **3** in Scheme 1 would have approximately the same free energy such that the equilibrium constant among these enzyme-bound forms would be *close to unity*.

Gerlt and Gassman (*4*) and Cleland and Kreevoy (*5*) proposed that the reduction of the kinetic barrier between **1** and **2** is achieved by the formation of a LBHB between His-95 and the incipient enediolate intermediate. In contrast to Albery and Knowles (*3*), Gerlt and Gassman (*4*) predict an equilibrium constant for the formation of **2** from either **1** or **3** to be *much less than unity* since the rate acceleration is due at least in part to the reduction of the intrinsic kinetic barriers[2] to these steps.

Formation of a short, very strong, LBHB in an enzyme−intermediate complex, or in a transition state, can provide an important contribution to catalysis (*4*, *5*). LBHB formation is favored by similar pK_a's of the two heteroatoms in the hydrogen bond, by a low dielectric constant, and by the absence of a competing hydrogen-bonding solvent such as water (*9*). A LBHB has been proposed to exist in the TIM reaction (*4*, *5*) on the basis of (i) the short hydrogen bond distance (2.7 Å) between neutral His-95 Nϵ and the O1 and O2 oxygens of the competitive inhibitor PGH in the X-ray structure of the TIM−PGH complex (*10*) and (ii) the possibility of matched pK_a's between neutral His-95 and the enediolate intermediate (*4*, *5*, *11*, *12*).

Short hydrogen bond distances involving enzymic carboxyl groups have been observed in X-ray crystal structures of citrate synthase with carboxyl or amide analogs of acetyl CoA (*13*) and in thermolysin and carboxypeptidase with intermediate analogs bound in the active site (*14*, *15*). Experimental evidence for the existence of LBHB's in solution was found using NMR to detect downfield chemical shifts ($\delta = 16-20$ ppm) and low fractionation factors[3] ($\phi \leq 0.4$) in serine proteases (*17*−*19*) and in the Δ^5-3-ketosteroid isomerase complex with dihydroequilenin, a tight binding analog of the dienolic intermediate (*20*−*22*). In these examples, the highly deshielded proton resonances with low fractionation factors, characteristic of LBHB formation, were found to involve enzymic carboxyl groups.

The present low-temperature, high-field protein NMR studies show that while His-95 donates a normal hydrogen bond to PGH, a highly deshielded resonance at 14.9 ppm is assigned to a LBHB from the NOH proton of bound PGH to the general-base catalyst Glu-165. The strong interaction of PGH NOH with Glu-165 in TIM suggests a dual role for Glu-165 in catalysis, namely proton transfer between the O1 and O2 oxygens as well as between the C1 and C2 carbons in the interconversion of DHAP and GAP. A preliminary abstract of this work has been published (*23*).

EXPERIMENTAL PROCEDURES

Materials. Yeast TIM, rabbit muscle α-glycerophosphate dehydrogenase (*sn*-glycerol-3-phosphate:NAD^+ 2-oxidoreductase; EC 1.1.1.8), glyceraldehyde-3-phosphate (GAP), reduced nicotinamide adenine dinucleotide (NADH), tri(monocyclohexylammonium) salt of phosphoglycolate (PGA),

[2] The intrinsic kinetic barrier is the activation barrier for proton transfer when the thermodynamic barrier for proton transfer is equal to zero [i.e. when ΔpK_a ($pK_a^{BH} - pK_a^{CH}$) = 0].

[3] The fractionation factor, ϕ, is defined as the equilibrium constant for replacement of a proton with a deuteron in a given system (*16*):

$$\phi = [E-D][H_2O]/[E-H][D_2O]$$

acetohydroxamic acid, Dowex-1-Cl, Dowex-50W-H^+, and DMSO-d_6 were from Sigma Chemical Co. (St. Louis, MO). Yeast TIM was found to be ≥95% pure as determined by 15% SDS−PAGE (*24*) with Coomassie Blue staining and densitometric analysis as well as by its specific activity which was 9000 units/mg with GAP as the substrate, using the assay described below. Deuterium oxide (D_2O, 99.96 atom % D) was from Aldrich (Milwaukee, WI). Tris-d_{11} and $^{15}NH_2$-OH−HCl were from Isotec, Inc. (Miamisburg, OH). The di(monocyclohexylammonium) salt of unlabeled phosphoglycolohydroxamic acid (PGH) was a gift from K. Collins. All solvents and reagents were of analytical or reagent grade and were used without further purification unless otherwise indicated. All solutions used in the NMR experiments were treated with Chelex-100 resin to remove trace paramagnetic metals and filtered through a 0.22 μm filter (Millipore) before addition to NMR samples.

H95N Mutant Yeast TIM Production. The expression vector containing the clone for the H95N mutant of yeast TIM was obtained as a gift from E. Komives and transformed into *Escherichia coli* strain DH5α. The bacterial transformant was grown in a final volume of 6 L of Luria−Bertani medium containing 200 mg/L ampicillin. Cells (35 mg) were harvested after 20 h by centrifugation for 15 min at 2000*g*. The cells were lysed by resuspension in lysis buffer (350 mL of 50 mM Tris-HCl buffer, pH 8.0, containing 5 mM EDTA, 10% sucrose, 1 mM DTT, 0.1% Triton X-100, and 0.1 mg/mL lysozyme) and stirring gently for 20 min followed by sonication; the lysate was centrifuged for 30 min at 20000*g* to remove cell debris. The ammonium sulfate fraction from 55% to 90% saturated was collected and dialyzed against TE buffer (10 mM Tris-HCl, pH 7.8, 1 mM EDTA). The crude protein was loaded onto a 150 mL column of Macro-Prep High Q Support (Bio-Rad, Hercules, CA) equilibrated in TE buffer and eluted with a linear gradient of 0−0.3 M NaCl in TE buffer (0.5 L to 0.5 L) at 2 mL/min. The H95N mutant TIM enzyme eluted near 0.1 M NaCl and was ≥95% pure as judged by densitometric analysis of Coomassie Blue stained 15% SDS−PAGE gels (*24*). The purified enzyme was concentrated by Centriprep and Centricon methods using the procedures provided by the supplier, Amicon (Danvers, MA).

The enzymatic activity was assayed by the conversion of GAP to DHAP coupled to glycerophosphate dehydrogenase and NADH by following the decrease in absorbance at 340 nm due to the oxidation of NADH to NAD^+ upon the addition of GAP. The coupled assay mixture contained 0.1 M Tris-HCl (pH 7.5), 5 mM EDTA, 1 unit of glycerophosphate dehydrogenase, 0.2 mM NADH, 10 mM glyceraldehyde-3-phosphate, and 1 μg of mutant enzyme. The k_{cat} of 35 units/mg and K_m of 3.5 mM obtained for yeast TIM H95N agrees with those previously reported (*25*).

Synthesis of ^{15}N-Labeled Phosphoglycolohydroxamic Acid (PGH). PGH was synthesized as described by Anderson et al. (*26*) for phosphonoacetohydroxamic acid with the following additions or modifications. A sample of the tri(monocyclohexylammonium) salt of phosphoglycolate (2.2 mmol) was dissolved in 3 mL of H_2O and converted to the free acid by passage through a 1.5 × 20 cm column of Dowex-50W-H^+. The fractions with pH values ≤4.0 were pooled and concentrated in a rotary evaporator with the water bath at 30 °C. The resulting clear oil was converted to the monoethyl ester by refluxing in 25 mL of absolute ethanol with 50 μL of 18 M H_2SO_4 for 4 h. The mixture was allowed to cool for 30 min and the ester was converted to the hydroxamic acid by adding 10 mL of a freshly prepared solution of 1.5 M $^{15}NH_2OH$−HCl (14.5 mmol) in 3.0 M NaOH. Water was added to dissolve any precipitate that formed, and the final pH was 12.4. After 30 min, the reaction mixture was diluted to 500 mL, titrated to pH 8.0 by dropwise addition of 10 M HCl, applied to a 1.5 × 23 cm column of Dowex 1-Cl, and washed with 100 mL of water. The column was eluted with a 0−0.1 M LiCl gradient in 20 mM HCl (325 mL to 325 mL) at 2 mL/min, and PGH eluted at 7−10 mM LiCl. PGH was located by ferric chloride assay (*7*). The Li^+ salt was recovered by lyophilization after titration to pH 8.0 with LiOH, and LiCl was removed by washing thoroughly with dry methanol−acetone (1:4). The yield of PGH (0.9 mmol) obtained in this way was 41% based on the starting quantity of PGA (6% based on $^{15}NH_2OH$−HCl) and behaved similarly to the unlabeled authentic PGH both in polyethyleneimine cellulose thin-layer chromotography, UV−visible spectroscopy, and NMR spectroscopy (*7*).

General NMR Methods. Unless otherwise stated, solution conditions for NMR studies were 0.6 mL of 0.3−0.7 mM (0.6−1.4 mM active sites) yeast wild type or H95N mutant TIM enzyme in 20 mM Tris-d_{11}-HCl buffer (pH 6.0, 7.5, or 9.0) with 100 mM NaCl and 10% (vol/vol) DMSO-d_6 and in the presence of 0−2.0 mM PGA or 0−2.0 mM PGH at −4.8 °C. The purified enzyme was exchanged into the buffer and salts by the Centricon method as described above. DMSO-d_6 was added to the system to permit lowering of the temperature to below 0 °C and for field/frequency locking. Its presence does not significantly affect the activity of these enzymes. The NMR data were collected on a Varian Unity Plus 600 MHz spectrometer using a Varian 5-mm triple resonance probe. Data were processed on a Silicon Graphics Personal IRIS 4D/35 Workstation using the FELIX software package (Biosym Technologies, Inc.). One-dimensional ^{1}H NMR data sets were collected using the 1331 pulse sequence (*27*) to avoid water excitation. The delays between the pulses were adjusted for maximum excitation at 14.9 ppm (i.e. 5800 Hz away from the carrier which is positioned at H_2O). The acquisition parameters included a 1.5-s relaxation delay, 512-ms acquisition time, and 26-μs 90° pulse width. Spectra were processed with 10 Hz line broadening and were zero-filled to 16 K before Fourier transformation. Multidimensional data sets were collected using the States-TPPI method (*28*) in all of the indirect dimensions, with relaxation delays of 0.9 s. The acquired domain data points were extended by one-third of the original size by the forward linear prediction routine in FELIX. Shifted (65−90°) sine bell filters were used in the first and subsequent dimensions, respectively, prior to zero-filling and Fourier transformation. The observed ^{1}H chemical shifts are determined with respect to the H_2O signal, which is 5.06 ppm downfield from external TSP at −4.8 °C and reported with respect to TSP. The ^{15}N chemical shifts are determined with respect to external $^{15}NH_4$-Cl (2.9 mM in 1 M HCl) at 20 °C, which is 24.93 ppm downfield from liquid ammonia (*29*) and are reported with respect to liquid ammonia.

^{1}H−^{15}N HMQC Spectra of ^{15}N-Labeled PGH and TIM−PGH. ^{1}H−^{15}N HMQC spectra were recorded using a pulse sequence in which the HMQC detection scheme was optimized to avoid water saturation (*30*). The data were

obtained at 600 MHz with spectral widths of 1600 and 8000 Hz in f_1 (^{15}N) and f_2 (^{1}H), respectively, and with 192 and 1024 complex points, respectively, in the t_1 and t_2 dimensions. A total of four transients were acquired for each hypercomplex t_1 point with ^{1}H and ^{15}N carriers positioned at 5.06 and 175 ppm, respectively. The final data matrix was 1024 × 1024 real points for the f_1 (^{15}N) and f_2 (^{1}H) dimensions, respectively.

^{15}N NMR Spectroscopy. 1D ^{15}N NMR was used to determine the limiting ^{15}N chemical shift value for anionic free [^{15}N]PGH by monitoring the pH dependence of the ^{15}N chemical shift of the hydroxylamine nitrogen resonance. The ^{15}N chemical shifts were referenced to external liquid ammonia as described (*31*). A Varian Unity-Plus 600 NMR spectrometer operating at 50.659 MHz for ^{15}N was used. Spectra were acquired without proton decoupling using a 5-mm broadband probe. The titrations were performed using samples which were 30 mM in free [^{15}N]PGH in H_2O at −4.8 and 20 °C by adding small amounts of 1 M NaOH to the sample. The acquisition parameters for the sample titration were as follows: spectral width, 12 001.2 Hz; acquisition time, 0.683 s; relaxation delay, 0.1 s; total number of transients, 512.

SS-NOESY Spectra of the TIM−PGH Complex. 2D NOESY spectra of the TIM−PGH complex were acquired with 50 ms mixing times using the SS-NOESY pulse sequence (*32*) to avoid excitation of the water resonance by the detection pulse. The maximum excitation of the SS pulse (140 μs) was adjusted to be 7143 Hz (11.9 ppm) from water. The sweep width was 16 000 Hz with 512 scans per FID and a recycle time of 1.5 s.

^{1}H NMR Titration of TIM with PGH. ^{1}H NMR titrations of yeast wild type TIM with PGH, were performed by adding small portions (6−66 μL) of a 20 mM stock solution of PGH (pH 7.5), prepared gravimetrically, to a 600 μL solution of 0.39 mM TIM (0.78 mM active sites). Since the complex of the reaction intermediate analog, PGH, with TIM is in slow exchange on the chemical shift time scale (see Results), the dissociation constant (K_d) for the complex could not be determined by following the changes in the ^{1}H chemical shifts. Therefore, the relative peak intensities (I_{obs}) for three well-resolved downfield resonances (δ = 14.9, 13.5, and 13.1 ppm) were determined by integrating the corresponding ^{1}H NMR peaks and plotted against the total concentration of PGH (L_{tot}) to determine K_d according to eq 1.

$$I_{obs} = I_{max}[(K_d + E_{tot} + L_{tot}) - ((K_d + E_{tot} + L_{tot})^2 - 4E_{tot}L_{tot})^{1/2}]/[2E_{tot}] \quad (1)$$

Determination of Proton Exchange Rates. Proton exchange rates with solvent for the His-95 NϵH proton in free (δ = 13.1 ppm) and PGH-bound yeast wild type TIM (δ = 13.5 ppm) and the PGH NOH proton (δ = 14.9 ppm) in PGH-bound yeast wild type TIM were determined from linewidth ($\Delta\nu_{1/2}$) measurements in ^{1}H NMR spectra over the temperature range −4.8 to 43 °C and were analyzed as Arrhenius plots according to eqs 2 and 3 (*33*)

$$\ln(1/T_{2obs}) = \ln[\exp(-E_d/RT + C_d) + \exp(-E_{ex}/RT + C_{ex})] \quad (2)$$

$$1/T_{2obs} = \pi\Delta\nu_{1/2} \quad (3)$$

where E_d is the activation energy for the dipolar ($1/T_{2d}$) and E_{ex} is the activation energy for the exchange (k_{ex}) contribution to the transverse relaxation rate. The two terms on the right side of eq 2 have unequal and opposite temperature dependences; $1/T_{2d}$ decreases with increasing temperature giving a positive slope because the dipolar correlation time is in the numerator of the relaxation equation, while k_{ex} increases with increasing temperature giving a negative slope equal to $-E_{ex}$, the activation barrier. The terms C_d and C_{ex} are the intercepts of the two lines at infinite temperature given by E_d and E_{ex}.

Mechanism-Based Prediction of Proton Exchange Rates. The rate constants for proton exchange with solvent (k_{ex}) needed to satisfy the observed extent of tritium transfer from substrate (DHAP) to product (GAP) and to solvent were computed for both intramolecular and intermolecular proton transfer mechanisms catalyzed by wild type and mutant TIM. Computer simulations of enzyme-catalyzed reactions were performed using a modification (*34*) of the program KINSIM (*35*). For intramolecular proton transfer, the mechanism of Scheme 1 was used with the addition of the kinetic steps for binding of DHAP (k_1, k_{-1}) and GAP (k_4, k_{-4}) and for exchange of tritium with solvent from Glu-165 in the enzyme−intermediate complex (k_{ex}). Values for the individual rate constants for the reaction of unlabeled DHAP were calculated as described by Raines et al. (*36*) from the parameters determined by tritium exchange−conversion experiments with wild type chicken TIM (*37*), yeast TIM (*1*), and E165D chicken TIM (*36*). Values for the individual rate constants for the reaction of trace concentrations of DHAP labeled with tritium were obtained from either the observed discrimination against solvent tritium incorporated into the products GAP (k_3) and DHAP (k_{-2}) or according to Swain et al. (*38*) from the experimental value for the primary deuterium kinetic isotope effect for the substrates DHAP (k_2) and GAP (k_{-3}). The specific radioactivity of the substrate at the start of the reaction (s_o) was taken as the ratio of the initial concentration of labeled DHAP to total DHAP. The specific radioactivity of the remaining substrate (s/s_o) during the progress of the reaction was expressed as a fraction of s_o. The specific radioactivity of the product (p) was taken as the ratio of the concentration of labeled GAP to total GAP, and the amount of tritium transferred from labeled DHAP to GAP during the progress of the reaction was expressed as the ratio p/s_o. Values of k_{ex} were systematically varied to obtain simultaneous correct values of s/s_o and p/s_o at the designated extent of reaction reported for each enzyme. The intermolecular transfer mechanism was modeled using the same values for the individual rate constants as described for the intramolecular mechanism with the following modifications.

The kinetic step for exchange of tritium with solvent from Glu-165 in the enzyme−intermediate complex (k_{ex}) was replaced with three kinetic steps describing the internal exchange of tritium from the enzyme-bound intermediate into an enzyme carrier group, from the enzyme carrier group into the intermediate, and for external exchange of tritium from the enzyme carrier group into solvent. The rate constant for external exchange was fixed to that observed in the present work, and the values for the internal exchange steps were computed, assuming them to be equal.

Determination of Fractionation Factor. Fractionation factors for His-95 NϵH and PGH NOH in PGH-bound yeast

wild type TIM were determined by integrating the corresponding ^{1}H NMR peaks at equilibrium in mixed H_2O-D_2O solutions (12, 27, 43, 58, 74, and 90% mole fraction H_2O) at −4.8 °C in the presence of 10% (vol/vol) DMSO-d_6 (*20*, *39*). Samples containing 0.34 mM TIM and 1.8 mM PGH in 20 mM Tris-d_{11}-HCl, pH(D) 7.5, with 100 mM NaCl were prepared by the addition of 60 μL of 3.8 mM yeast wild type TIM and 12 μL of 100 mM PGH, each in 22 mM Tris-d_{11} (pH 7.5) and 111 mM NaCl, to 528 μL of weighed fractions of H_2O- and D_2O-containing buffers of the same composition and pH(D) and 65 μL of DMSO-d_6 as described by Schowen and Schowen (*16*). The NMR tubes were incubated at 4 °C for 1 h before NMR experiments which is >6000 half-times for exchange of the slowest exchanging downfield resonance. Accordingly, no changes in the intensities of His-95 NϵH (δ = 13.5 ppm) and PGH NOH (δ = 14.9 ppm) proton resonances were seen after 24 h at 4 °C. The fractionation factors from the NMR-derived data were determined with nonlinear least squares fits to eq 4:

$$I = I_{max}(X)/(\phi(1 - X) + X) \quad (4)$$

where I is the peak integral, X is the mole fraction H_2O, and I_{max} is the peak integral at 100% H_2O. Relative peak intensity was determined by normalizing peak integrals, I, to I_{max}.

RESULTS

Assignment of Deshielded Proton Resonances of TIM. The low-field region of the ^{1}H NMR spectra for free yeast wild type TIM and its complexes with the intermediate analogs PGH and PGA are shown in Figure 1. Free TIM showed a well-resolved resonance at 13.1 ppm and less well-resolved resonances near 11.3 and 11.2 ppm (Figure 1A). The fully saturated TIM−PGH complex showed well-resolved signals at 14.9 and 13.5 ppm and less well-resolved signals at 12.3, 11.9, 11.8, 11.4, 11.3, and 10.9 (Figure 1B). These low-field signals in the spectrum of the TIM−PGH complex did not change in chemical shift or line width over the pH range 6−9 (data not shown). The TIM−PGA complex showed a well-resolved signal at 13.3 ppm and less well-resolved signals near 12.0, 11.9, 11.6, 11.3, 11.2, and 10.9 ppm (Figure 1C). Notably, in the TIM−PGA complex (Figure 1C), the resonance at 14.9 and 12.3 ppm are absent and the resonance to 10.9 ppm is much weaker in comparison with the TIM−PGA complex (Figure 1B), suggesting the NOH and NH protons of PGH to be two of these signals (see below).

Figure 1 also shows the low-field region of the ^{1}H NMR spectrum for the free H95N mutant of yeast TIM and its complex with PGH. Free H95N TIM showed no signal at 13.1 ppm but a well-resolved signal at 12.2 ppm and less well-resolved signals near 11.6, 11.4, 11.3, and 11.1 ppm (Figure 1D). The H95N TIM−PGH complex showed no signal at 13.5 ppm but well-resolved signals at 14.1 and 12.4 ppm and less well-resolved signals near 11.6, 11.3, 11.2, and 11.1 ppm (Figure 1E).

The resonance at 13.5 ppm in the TIM−PGH complex (Figure 1B) has been rigorously assigned to the NϵH of His-95 on the basis of its presence in the "His-95-only" (H103Q + H185Q) mutant and by its 98 Hz coupling to specifically labeled ^{15}Nϵ of His-95 (*40*). It has been shown that His-95

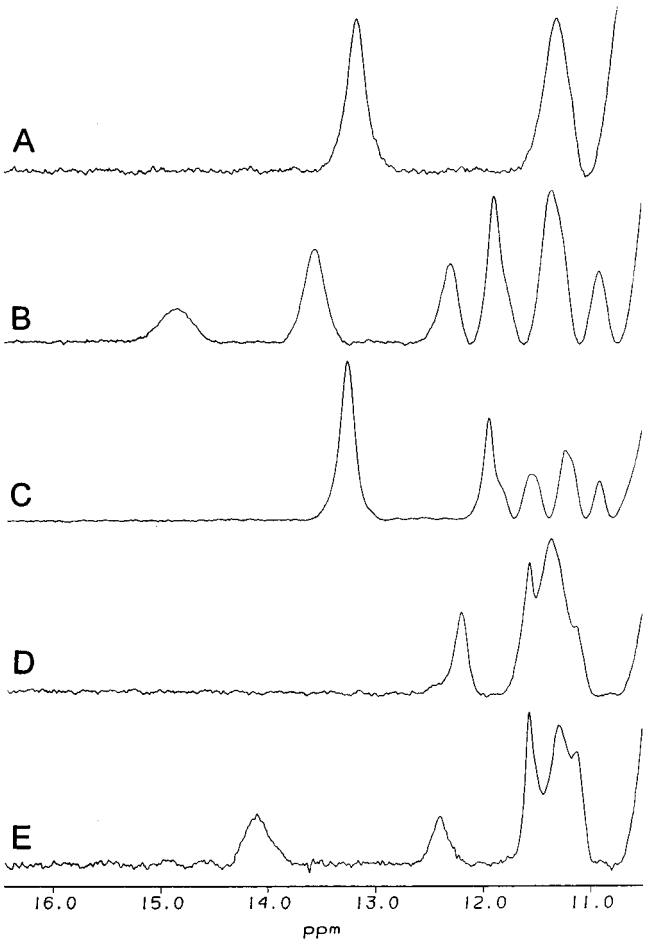

FIGURE 1: Low-field region of 600 MHz ^{1}H NMR spectra of yeast TIM. (A) Free wild type enzyme (1.0 mM). (B) Complex of wild type enzyme (1.0 mM) with 2.0 mM PGH. (C) Complex of wild type enzyme (1.2 mM) with 2.0 mM PGA. (D) Free H95N mutant TIM (0.6 mM). (E) Complex of H95N mutant TIM (0.6 mM) with 2.0 mM PGH. All concentrations of TIM are given in subunits. Other components present were 20 mM Tris-d_{11}-HCl, pH 7.5, 100 mM NaCl, and 10% (vol/vol) DMSO-d_6. T = −4.8 °C. Spectra were obtained as described in Experimental Procedures.

exists as the neutral Nϵ-protonated form in both the free and PGH-bound enzyme (*11*). The disappearance of the signal at 13.1 ppm in the H95N mutant (Figure 1D) and at 13.5 ppm in the H95N TIM-PGH complex (Figure 1E) confirms the loss of His-95.

The presence of a resonance at 12.2 ppm in the free H95N mutant which shifts to 12.3 ppm in the PGH complex (Figures 1D and 1E) suggests that this resonance comes from the protein both in the mutant and wild type enzymes. Such an assignment to an NH resonance of the protein is consistent with its slow exchange with solvent (see below). The broad resonance at 14.1 ppm in the H95N−PGH complex (Figure 1E) likely corresponds to the broad 14.9 ppm signal in the PGH complex of the wild type enzyme (Figure 1B).

The absence of the most downfield resonance near 14.9 ppm in the TIM−PGA complex (Figure 1C), which does not contain the NH or NOH group, is consistent with the assignment of the resonance at 14.9 ppm in the TIM−PGH complex (Figure 1B) to either the 1-NH or 1-NOH proton of enzyme-bound PGH. The decreased intensity of the resonance at 10.9 ppm in the TIM−PGA complex is consistent with assignment of the other hydroxamic acid

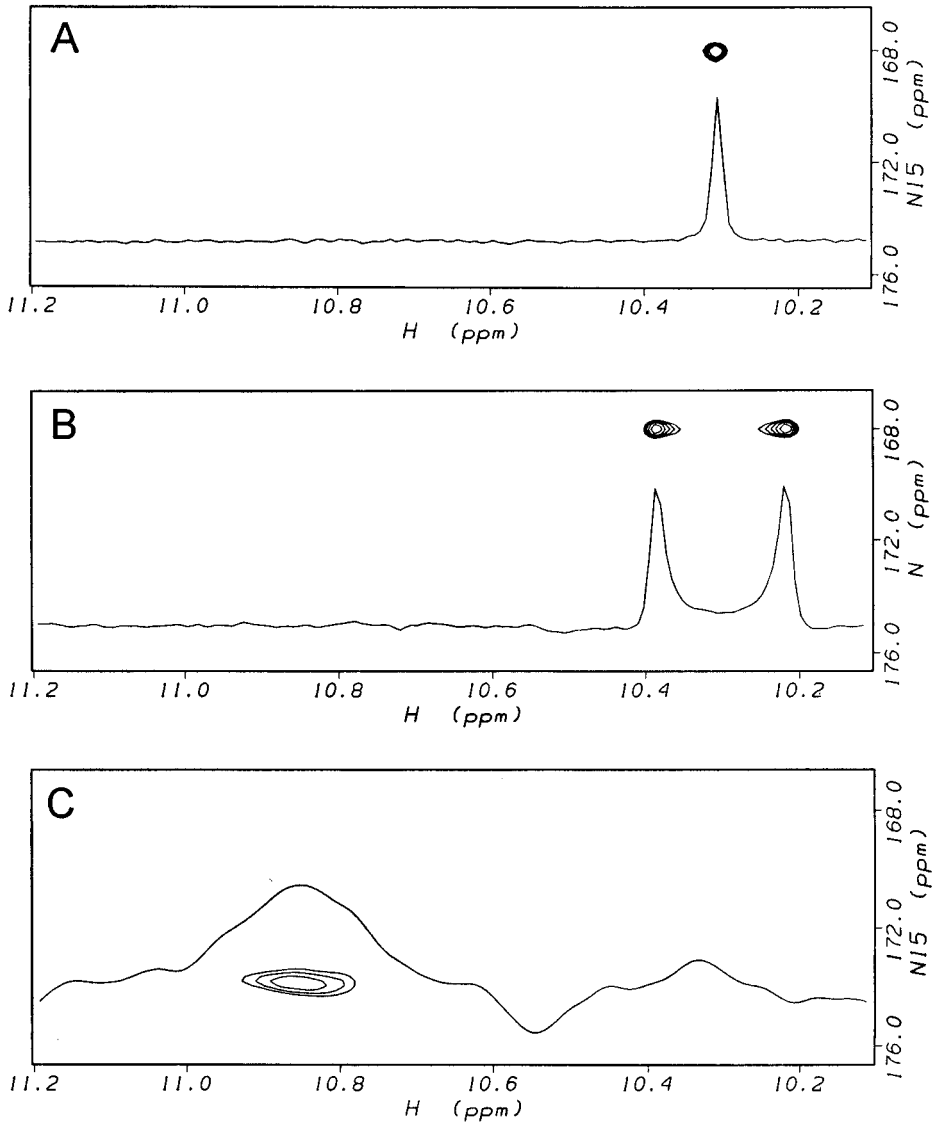

FIGURE 2: Two-dimensional $^1H-^{15}N$ HMQC spectra of free [^{15}N]PGH and the [^{15}N]PGH−TIM complex. The $^1H-^{15}N$ HMQC spectrum of 30 mM free [^{15}N]PGH in H_2O and 10% (vol/vol) DMSO-d_6 at pH 4.9 with (A) and without (B) ^{15}N decoupling. (C) $^1H-^{15}N$ HMQC spectrum with ^{15}N decoupling of enzyme-bound [^{15}N]PGH. In spectrum C, the sample contained 0.7 mM yeast TIM subunits, 2.0 mM [^{15}N]PGH, and the other components and conditions are given in Figure 1. One-dimensional slices through the cross peaks in the proton dimension of the $^1H-^{15}N$ HMQC spectra are also shown. Spectra were obtained as described in Experimental Procedures.

proton to $\delta = 10.9$ ppm. In the X-ray structure of the TIM−PGH complex (*10*), the two carboxyl oxygens of Glu-165 are within close hydrogen bonding distance to the PGH N1 nitrogen (2.51 and 2.66 Å in the two subunits) and the O1 oxygen (2.68 and 3.08 Å in the two subunits), suggesting that both of these proton resonances should be deshielded.

To clarify the assignments of the PGH NH and NOH proton resonances, 2D $^1H-^{15}N$ HMQC spectroscopy was used to determine the ionization state and tautomeric form of free and enzyme-bound PGH. For these experiments, ^{15}N-enriched PGH was synthesized. The 2D NMR method correlates the ^1H and ^{15}N chemical shifts of directly bonded $^1H-^{15}N$ pairs by selecting for the large $^1H-^{15}N$ scalar coupling ($^1J_{N-H} \sim 90$ Hz) (*41*, *42*). A $^1H-^{15}N$ HMQC spectrum will yield a single cross peak for the 1-^{15}NH proton of specifically labeled [^{15}N]PGH which will be split to a doublet according to its $^1J_{N-H}$ value. In addition to providing the ^1H and ^{15}N chemical shifts, the HMQC experiments also, under favorable conditions, provide the $^1J_{N-H}$ value for PGH.

Figure 2A shows $^1H-^{15}N$ HMQC spectra of free [^{15}N]-PGH at pH 4.9 with ^{15}N decoupling. A single $^1H-^{15}N$ cross peak was observed with ^1H and ^{15}N chemical shft values $\delta(^1H) = 10.3$ ppm and $\delta(^{15}N) = 168$ ppm. Without ^{15}N decoupling (Figure 2B) a doublet is seen with $^1J_{N-H} = 102$ Hz in free [^{15}N]PGH. Scheme 2 shows the tautomeric and resonance forms of neutral and anionic PGH ($pK_a = 9.5$) (*7*) in which a proton either is or is not directly bonded to the nitrogen. The observation of a $^1H-^{15}N$ cross peak indicates that the nitrogen in the neutral form of free PGH is predominantly in the protonated form (**4a,b**) at pH 4.9. The $^1H-^{15}N$ hydroxamate cross peak was not detectable at pH values ≥ 6.0 presumably due to hydroxide-catalyzed exchange broadening. A limiting ^{15}N chemical shift value of $\delta(^{15}N) = 183$ ppm for anionic free [^{15}N]PGH was determined by monitoring the pH dependence of the ^{15}N chemical shift using direct ^{15}N NMR spectroscopy, indicating an overall $\Delta\delta(^{15}N)$ of 15 ppm from the neutral to anionic form (data not shown). It has been reported that the anionic

Scheme 2

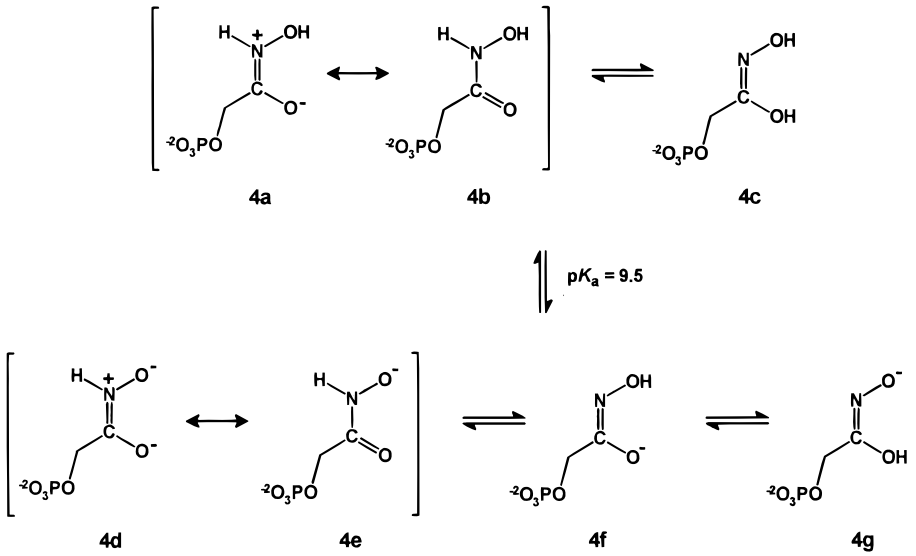

form of PGH in solution is a mixture of forms **4d,e** and **4f** but not **4g** (Scheme 2) (*43*).

The ^{1}H−^{15}N cross peak in the 2D HMQC spectrum of the TIM−[^{15}N]PGH complex with ^{15}N decoupling (Figure 2C) gives ^{1}H and ^{15}N chemical shift values of $\delta(^1H) = 10.9$ ppm and $\delta(^{15}N) = 174$ ppm. The ^{1}H chemical shift value for the ^{1}H−^{15}N cross peak in the TIM−[^{15}N]PGH complex is independent of pH in the range 6−9. At 13 °C and above, the ^{1}H−^{15}N cross peak was not detected presumably due to exchange broadening. The observation of ^{1}H−^{15}N coupling as indicated by the cross peak in the TIM−[^{15}N]PGH complex provides evidence that enzyme-bound PGH is in the NH neutral (**4a,b**) or anionic (**4d,e**) form on the enzyme (Scheme 2). The relatively small change in the ^{1}H chemical shift ($\Delta\delta = 0.7$ ppm) for the NH of PGH upon binding TIM suggests that this proton is involved in a normal hydrogen bond. The large increase in the ^{15}N chemical shift value from 168 to 174 ppm, which is halfway toward complete ionization, indicates a resonance form of enzyme-bound PGH with a significant amount of N1═C2 double bond character (**4a** or **4d**, Scheme 2).

While the H−N1 bond of enzyme-bound PGH is intact, the NO−H bond may be weakened or partially broken. The chemical shift assignment of the NH proton of enzyme-bound PGH of 10.9 ppm indicates that the resonance at 14.9 ppm in the TIM−PGH complex (Figure 1B), which is absent in the TIM−PGA complex (Figure 1C), comes from the 1-NOH proton. Consistent with this assignment, SS-NOESY spectra reveal proximity of the 14.9 ppm resonance to His-95 (Figure 3). Figure 3A shows equally strong NOE's (S/N = 5.6) from the NϵH of His-95 (at 13.51 ppm) to both its CϵH (at 7.54 ppm) and its CδH (at 6.76 ppm) as expected for the neutral Nϵ-protonated form. Figure 3B shows weak and approximately equal NOE's (S/N = 2.7) from His-95 CϵH (at 7.54 ppm) and His-95 CδH (at 6.76 ppm) to the 14.9 ppm resonance. The appearance of the highly deshielded proton resonance at 14.9 ppm in ^{1}H NMR spectra of the TIM−PGH complex is consistent with partial transfer of the 1-NOH proton of enzyme-bound PGH to the carboxylate group of Glu-165; proton chemical shift values for −COOH groups in organic solvents are ∼12 ppm (*44*).

An estimate of the ^{1}H chemical shift value for the 1-NOH of unbound PGH was obtained from ^{1}H NMR spectra of

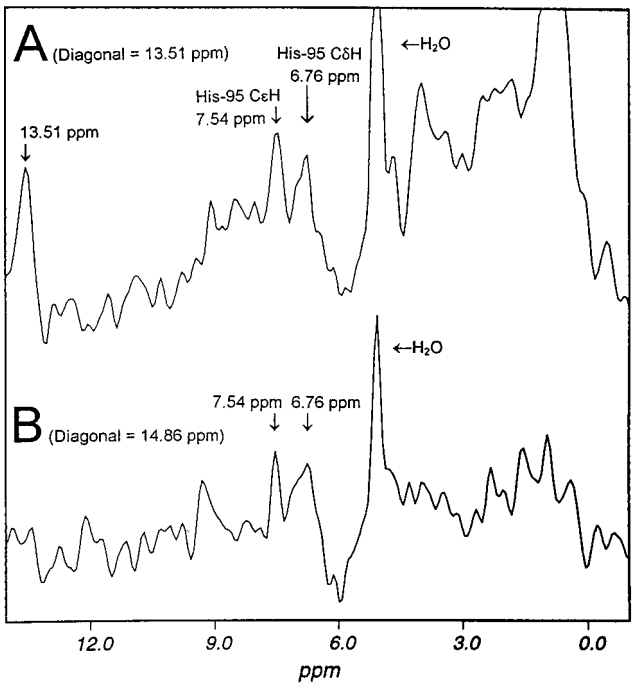

FIGURE 3: Two-dimensional SS-NOESY studies of the TIM−PGH complex. One-dimensional slices through the diagonal cross peaks in the t_1 dimension of the NϵH proton resonance of His-95 at 13.51 ppm (A) and the proton resonance at 14.86 ppm (PGH NOH) (B). The sample contained 0.7 mM yeast TIM subunits, 2.0 mM [^{15}N]PGH, and the other components and conditions are given in Figure 1. Spectra were obtained as described in Experimental Procedures.

500 mM acetohydroxamic acid (**6**) in dry DMSO-d_6 at 26.8

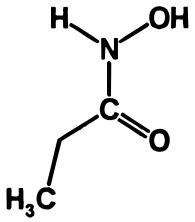

6

°C (data not shown). The absence of solvent exchange with protons allowed the observation of downfield resonances at

Table 1: Deshielded Proton Resonances in the Yeast Triosephosphate Isomerase−PGH Complex[a]

δ (ppm)	assignment	interaction	$\Delta\delta$ (ppm)	ϕ	$(k_{ex}^{obsd})^b$ (s^{-1})	$(k_{ex}^{intrinsic})^{b,c}$ (s^{-1})	protection factor[b]
14.9	PGH NOH	Glu-165	6.2	0.38	3900	3500	∼1
13.5	His-95 NϵH	PGH O2	0.4	0.71	80	3500	44
10.9	PGH NH	Glu-165	0.7	nd	nd	3500	nd

[a] Conditions are 20 mM Tris-d_{11}-HCl, pH 7.5, 100 mM NaCl, 10% (vol/vol) DMSO-d_6, and $T = -4.8$ °C. [b] $T = 30$ °C. [c] Calculated according to Eigen (*45*) for the acid- or base-catalyzed exchange of labile protons at pH 7.5 using pK_a values of ≥11 for neutral His-95 NϵH (*11*) and 9.5 for PGH NOH and NH (*7*).

10.4 and 8.7 ppm for the 1-NH and the 1-NOH protons, respectively. The resonance at 10.4 ppm is assigned to the 1-NH proton of acetohydroxamic acid on the basis of the observation of a doublet ($J = 98$ Hz) due to the presence of ^{15}N at natural abundance and is similar to the $\delta(^1H) = 10.2$ ppm for the 1-NH of PGH. The resonance at 8.7 ppm is assigned to the 1-NOH proton of acetohydroxamic acid and broadens upon the addition of water due to rapid exchange. Thus, the interaction of the 1-NOH proton of PGH with the carboxyl group of Glu-165 deshields the 1-NOH proton by ∼6.2 ppm ($\Delta\delta \approx 14.9-8.7$ ppm) upon binding to TIM. Table 1 summarizes the assignments and properties of the deshielded proton resonances in the yeast TIM−PGH complex.

^{1}H NMR Titration of TIM with PGH. In a titration of yeast wild type TIM with PGH, resonances of both free TIM and TIM−PGH are seen, indicating slow exchange of these two forms on the ^{1}H chemical shift time scale at −4.8 °C (data not shown). A titration monitoring the relative peak intensity (*I*) values for the disappearance of the 13.1 ppm resonance and appearance of the 13.5 and 14.9 ppm resonances upon addition of PGH to TIM was fit to eq 1 yielding a stoichiometry of 1.0 PGH molecule bound per enzyme subunit with a $K_d = 6.3 \pm 1.7$ μM at −4.8 °C (Figure 4). This value is slightly tighter than the kinetically determined K_i value of 15 ± 3 μM for PGH as a competitive inhibitor of yeast wild type TIM at 30 °C (*1*) suggesting a negative $\Delta H°$ for the binding of PGH.

Exchange Properties of the Deshielded Protons of TIM. The temperature dependences of the line widths of the downfield resonances were monitored by ^{1}H NMR spectra for yeast wild type TIM in the absence and presence of saturating PGH. Arrhenius plots are shown for the His-95 NϵH proton in free ($\delta = 13.1$ ppm) (Figure 5A) and PGH-bound yeast wild type TIM ($\delta = 13.5$ ppm) (Figure 5B) and for the PGH NOH proton ($\delta = 14.9$ ppm) in PGH-bound yeast wild type TIM (Figure 5C). The resonance width of the His-95 NϵH proton at 13.1 ppm in free TIM decreases with increasing temperature over the range −4.8 to 19 °C, indicating a predominant dipolar ($1/T_{2d}$) contribution to line width, and increases with increasing temperature above 19 °C, indicating a predominant exchange (k_{ex}) contribution to line width (Figure 5A). Analysis of the temperature dependence of the resonance width of the 13.1 ppm signal in free TIM according to eqs 2 and 3 yields activation energies for $1/T_{2d}$ and k_{ex} of -4.3 ± 0.8 kcal/mol and 14.7 ± 0.9 kcal/mol, respectively. The temperature dependence of k_{ex} (Figure 5A) yields a value for the first-order exchange rate with solvent at 30 °C of 79 s^{-1} for the His-95 NϵH proton in free TIM. This rate is 44-fold slower than the exchange rate of an exposed histidine (Table 1), consistent with its participation in a hydrogen bond. The X-ray structure of free TIM shows His-95 to be hydrogen bonded to Glu-165 at a distance of 3.3 Å (*46*).

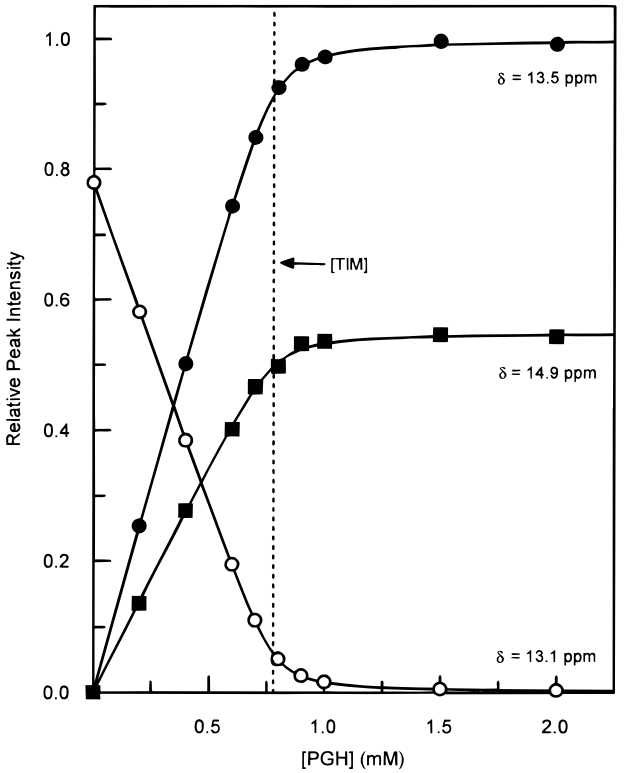

FIGURE 4: ^{1}H NMR titration of yeast TIM (0.78 mM) with PGH. The decrease in the relative peak intensity of the His-95 NϵH proton in free TIM ($\delta = 13.1$ ppm) (○) and increase in the relative peak intensities of the His-95 NϵH proton in PGH-bound TIM ($\delta = 13.5$ ppm) (●) and the PGH NOH proton in enzyme-bound PGH ($\delta = 14.9$ ppm (■) were followed in ^{1}H NMR spectra as the enzyme was titrated with PGH. The curves were generated by eq 1 using dissociation constants $K_d = 5.0 \pm 0.9$ μM (○), $K_d = 6.5 \pm 0.5$ μM (●), and $K_d = 7.5 \pm 1.7$ μM (■), which yield a mean value of $K_d = 6.3 \pm 1.7$ μM for the binding of PGH to the enzyme. The vertical dotted line represents the concentration of enzyme active sites (0.78 mM). For all curves, the binding stoichiometry is 1.0 per subunit.

Figure 5B shows that the resonance width of the His-95 NϵH signal ($\delta = 13.5$ ppm) in the TIM−PGH complex also decreases with increasing temperature over the range −4.8 to 19 °C and then begins to increase at higher temperatures. Analysis of the temperature dependence of the His-95 NϵH resonance in the TIM−PGH complex yields values of $E_d = -4.3 \pm 0.6$ kcal/mol for the dipolar contribution and $E_{ex} = 19.1 \pm 1.9$ kcal/mol for the exchange contribution to $1/T_{2obs}$. Thus the energy of activation for proton exchange of His-95 NϵH has increased by 4.4 kcal/mol in the PGH complex. The temperature dependence of k_{ex} yields a value of 80 s^{-1} at 30 °C for the His-95 NϵH proton in PGH-bound TIM which is 44-fold slower than the exchange rate of an exposed histidine (Table 1) consistent with hydrogen bonding. The X-ray structure of the TIM−PGH complex (*10*) shows His-95 to donate a hydrogen bond to O1 and O2 of PGH at

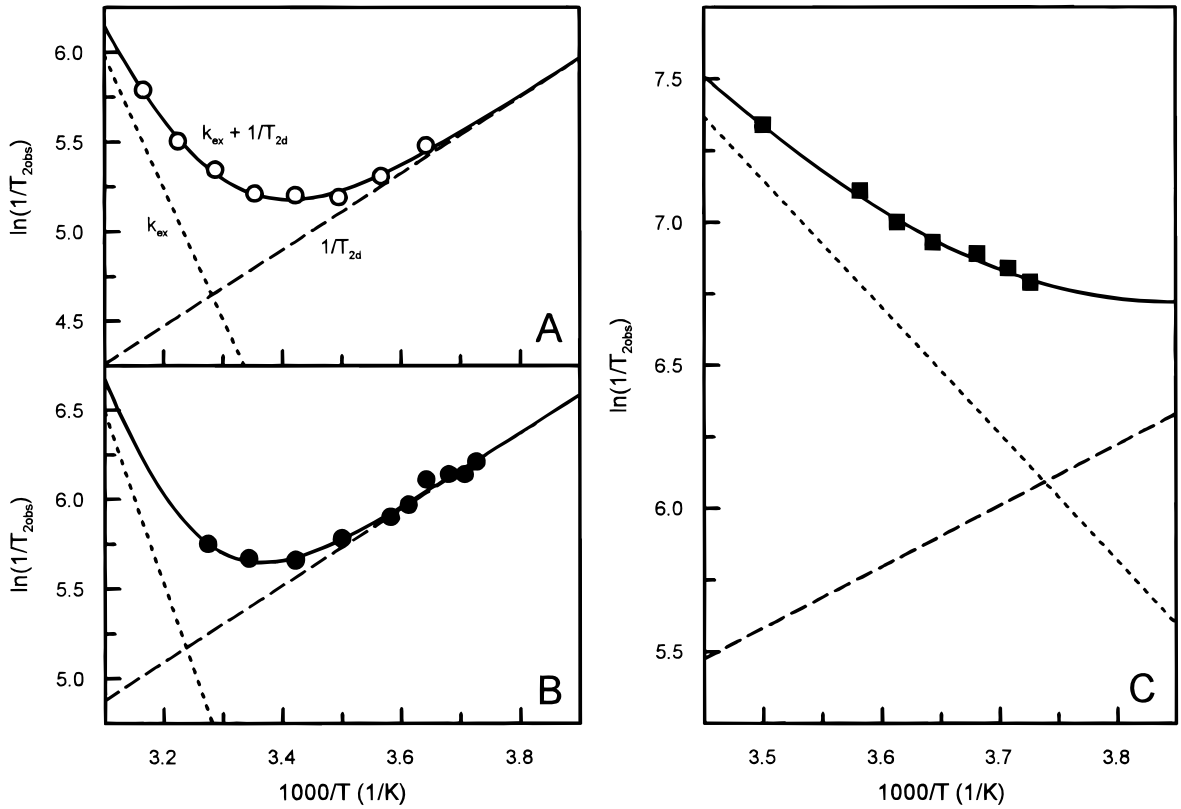

FIGURE 5: Arrhenius plots of the effect of temperature on the observed transverse relaxation rate ($1/T_{2obsd}$) of downfield proton resonances in free and complexed TIM. (A) His-95 NϵH proton signal (δ = 13.1 ppm) in free TIM. (B) His-95 NϵH proton signal (δ = 13.5 ppm) in PGH-bound TIM. (C) PGH NOH proton signal (δ = 14.9 ppm) in enzyme-bound PGH. Concentrations of components and conditions are as in Figure 1. The dotted line in each panel represents the exchange contribution (k_{ex}) to $1/T_{2obs}$, and its slope and *y*-intercept are given by the activation energy (E_{ex}) and Arrhenius coefficient (C_{ex}), respectively. The dashed line in each panel represents the dipolar contribution ($1/T_{2d}$) to $1/T_{2obs}$, and its slope and *y*-intercept are given by E_d and C_d, respectively. The curve through the data in each panel represents the composite results for both the k_{ex} and $1/T_{2d}$ contributions to $1/T_{2obs}$ and is described by eqs 2 and 3 using E_{ex} = 14.7 ± 0.9 kcal/mol, C_{ex} = 28.8 ± 1.5, E_d = −4.3 ± 0.8 kcal/mol, and C_d = −2.36 ± 0.30 (○); E_{ex} = 19.1 ± 1.9 kcal/mol, C_{ex} = 36.2 ± 1.5, E_d = −4.3 ± 0.6 kcal/mol, and C_d = −1.74 ± 0.20 (●); and E_{ex} = 8.9 ± 0.3 kcal/mol, C_{ex} = 22.7 ± 0.5, E_d = −4.3 kcal/mol, and C_d = −1.89 (■).

average distances of 3.12 and 2.66 Å, respectively. The activation barrier for the dipolar contribution to $1/T_2$ of −4.3 kcal/mol was found for the 13.5 ppm signal (Figure 5B), in good agreement with that of the 13.1 ppm signal (Figure 5A).

Figure 5C shows that the resonance width of the 1-NOH proton of enzyme-bound PGH (δ = 14.9 ppm) increases with increasing temperature and becomes undetectably broad above 15 °C so that exchange is the predominant contribution to line width. Because the line width could not be measured at lower temperatures where dipolar contributions to the line width contribute more, values of E_{ex} and C_{ex} were obtained from a fit of the data to eqs 2 and 3 using the fixed value of E_d = −4.3 kcal/mol and differing fixed values of C_d. The data were best fit with an E_{ex} = 8.9 ± 0.3 kcal/mol for k_{ex}. The temperature dependence of k_{ex} of the 1-NOH proton yields a value of 3900 s^{-1} at 30 °C which yields a protection factor of ∼1.0 when compared to that of free PGH (Table 1). The reason for this small protection factor is that this rate may reflect the rate of dissociation of the TIM−PGH complex[4] (see Discussion).

[4] The rate of 3900 s^{-1} at 30 °C does not violate the slow exchange of the TIM−PGH complex on the chemical shift time scale of <1500 s^{-1} at −4.8 °C, as calculated from the $\Delta\delta$ of 0.4 ppm for His-95 NϵH. From the activation energy of 8.9 kcal/mol, this upper limit increases to $<10^4$ s^{-1} at 30 °C.

The resonance widths of the downfield protein signals at 12.3, 11.9, 11.8, 11.4, 11.3, and 10.9 ppm in ^{1}H NMR spectra of the TIM−PGH complex all decreased with increasing temperature over the entire range that could be studied from −4.8 to 30 °C, showing no exchange contribution to $1/T_{2obs}$. Hence, the exchange rates of these resonances are much slower than ∼200 s^{-1} on the basis of their line widths at 30 °C, consistent with the behavior of slowly exchanging NH protons of the protein. Indeed the resonance at 12.3 ppm showed little exchange with D_2O after 8 h of incubation at 4 °C. The large k_{ex} of 3900 s^{-1} for the 1-NOH resonance at 30 °C compared to 80 s^{-1} for the His-95 NϵH proton in PGH-bound TIM and to ≪200 s^{-1} for the other downfield resonances provides further evidence for the assignment of the 14.9 ppm signal to the 1-NOH proton of enzyme-bound PGH.

The temperature dependence of the line width of the 1-NH resonance of enzyme-bound PGH of the TIM−PGH complex (δ = 10.9 ppm) could not be analyzed because of an overlapping protein resonance with a slowly-exchanging proton at the same chemical shift. However, ^{1}H−^{15}N HMQC spectra show that the ^{1}H−^{15}N cross peak from the 1-^{15}NH proton of enzyme-bound [^{15}N]PGH (δ = 10.9 ppm), like the 14.9 ppm signal, broadens and becomes undetectable above 15 °C. The disappearance of both the 1-NH and 1-NOH resonances above 15 °C indicates similar exchange

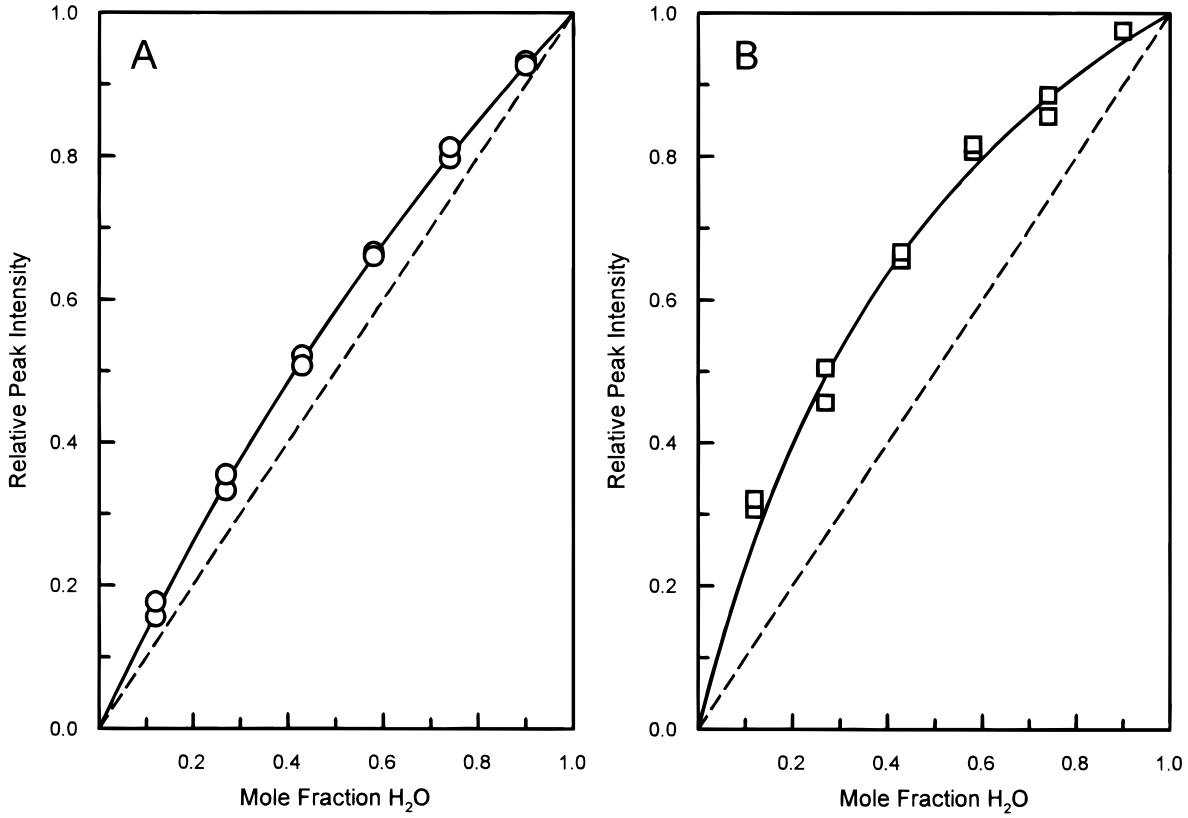

FIGURE 6: Determination of the fractionation factors of downfield proton resonances in the TIM−PGH complex. Plot of the relative peak intensity of the (A) His-95 NϵH proton signal (δ = 13.5 ppm) in PGH-bound TIM and of the (B) PGH NOH proton signal (δ = 14.9 ppm) in enzyme-bound PGH as a function of the mole fraction H_2O in the aqueous solution. Components and conditions are otherwise as given in Figure 1. The curve in each panel is described by eq 4 using (A) $\phi = 0.71 \pm 0.02$ and (B) $\phi = 0.38 \pm 0.06$; the dashed line in each panel is drawn for $\phi = 1$.

rates which would be expected for the two hydroxamic acid protons (Scheme 2).

Fractionation Factors of the Deshielded Protons of TIM. Strong hydrogen bonds characteristically have low fractionation factors[3] (*47*). Fractionation factors (ϕ) for His-95 NϵH and PGH NOH in PGH-bound yeast wild type TIM at equilibrium were determined by the intensities of the ^{1}H NMR signals in titrations in which the mole fractions of H_2O and D_2O in the system were systematically varied. A fit to eq 4 of the titration data of plots of the His-95 NϵH (Figure 6A) and PGH NOH (Figure 6B) signal intensity as a function of the mole fraction H_2O yielded a fractionation factor of $\phi = 0.71 \pm 0.02$ for His-95 NϵH and $\phi = 0.38 \pm 0.06$ for PGH NOH (Table 1). These results are consistent with a normal hydrogen bond involving His-95 and an unusually strong hydrogen bond involving the 1-NOH proton of PGH. Because of spectral overlap or slow exchange, reliable fractionation factors for the other deshielded resonances could not be obtained.

DISCUSSION

X-ray Structure of the TIM−PGH Complex. The X-ray structure of the complex of TIM with PGH (Figure 7A) (*10*) approximates the structure of the enzyme−intermediate complex which results from the deprotonation of DHAP or GAP, with the hydroxylamine nitrogen replacing C1. Like the *cis*-enediol(ate) intermediate in which the O1−C1=C2−O2 atoms are coplanar (**2**, Scheme 1), PGH is bound in a *cis* conformation in which the hydroxamic acid hydroxyl group, the imidate group, and the phosphate ester oxygen are coplanar. From this structure it is apparent that Glu-165, with its carboxyl group positioned above the plane of the O1−N1−C2 atoms in PGH with carboxyl O to N distances of 2.51 and 2.66 Å in the two subunits, and carboxyl O to C2 distances of 3.30 and 3.37 Å, is well positioned for proton transfer between the C1 and C2 carbons of the enediol(ate) intermediate. The other carboxyl oxygen of Glu-165 approaches O1 of PGH at distances of 2.68 and 3.08 Å in the two subunits. His-95 is positioned between the O1 and O2 oxygens of PGH with average distances of 3.12 and 2.66 Å, respectively, suggesting that this residue is responsible for polarizing the substrate carbonyl groups and possibly shuttling protons between the two oxygens of the enediol(ate) during the isomerization reaction. Lys-12 creates a positive environment in the active site so that the phosphodianion substrate can bind (*48*). Although the X-ray structure of the TIM−PGH complex provides a clear picture of the functional groups available for catalysis, it does not provide information regarding the mechanistic sequence of events.

NMR-Modified Structure of the TIM−PGH Complex. NMR studies of the TIM−PGH complex provide information on the chemical properties of specific atoms (i.e. chemical shift values, proton exchange rates with solvent, and fractionation factors). Figure 7A shows the structure of the TIM active site with bound PGH as inferred from X-ray studies (*10*), and Figure 7B shows a modified structure of this complex on the basis of the NMR studies. Specific changes include the following:

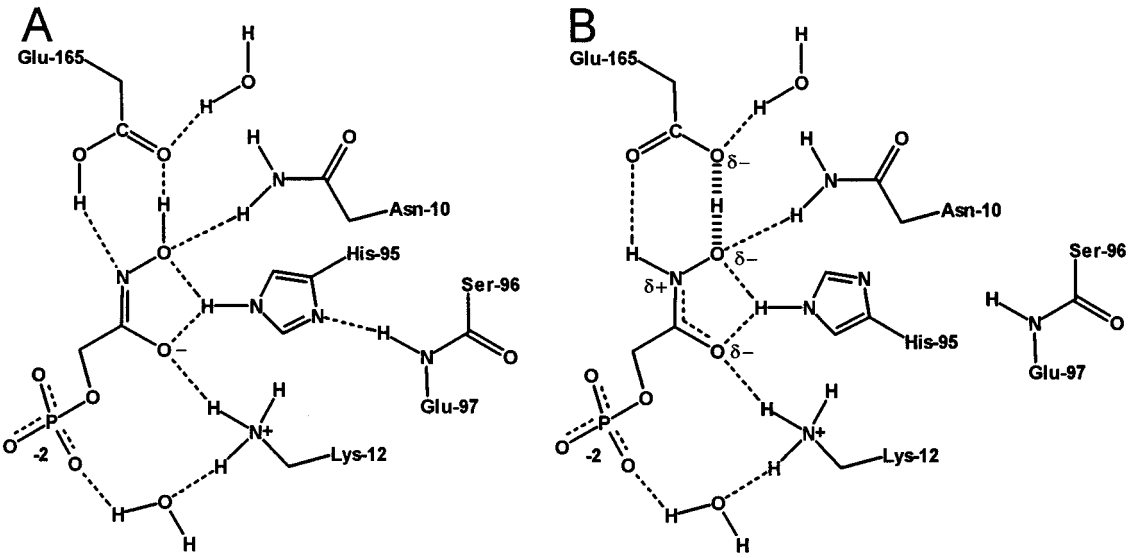

FIGURE 7: Comparison of the (A) X-ray structure of the TIM−PGH complex (*10*) with (B) the NMR-modified structure of the TIM−PGH complex.

(i) An LBHB occurs between the 1-NOH proton of PGH and a carboxyl oxygen of the general base-catalyst, Glu-165, on the basis of the ~6.2 ppm downfield shift of the 1-NOH proton resonance (Figure 1) and its low fractionation factor, $\phi = 0.38$ (Figure 6). Although the strength of this hydrogen bond is difficult to measure, its length is short. In crystals of small molecules studied by both high resolution X-ray diffraction and solid-state NMR, McDermott and Ridenour (*49*) have found a strong correlation of OH···O hydrogen bond distances (D) with chemical shifts (δ) of the protons in 59 hydrogen bonds. These data were found by empirical least squares methods to be well fit by eq 5 (*21*):

$$D = 5.04 - 1.16 \ln \delta + 0.0447\delta \qquad (5)$$

where D is expressed in Å and δ is ppm. From this correlation, using eq 5, the chemical shift of 14.86 ppm for the PGH NOH···Glu-165 hydrogen bond corresponds to a distance of 2.57 ± 0.05 Å. This distance overlaps with the shorter of the two PGH NOH···Glu-165 hydrogen bond distances in the two subunits of the crystalline yeast TIM−PGH complex, which were 2.68 ± 0.2 and 3.08 ± 0.2 Å. Hence, *in solution*, the detection of only a single downfield chemical shift for the PGH NOH···Glu-165 hydrogen bond suggests equal and short hydrogen bond distances on both subunits.

(ii) The H-N1 bond of enzyme-bound PGH is intact on the basis of the observation of $^{1}H-^{15}N$ coupling, and this proton is involved in a normal hydrogen bond to Glu-165 as indicated by the relatively small downfield shift of 0.6 ppm for the NH proton of PGH upon binding TIM (Figure 2). The bond structure and protonation state of the carboxyl group of Glu-165 is modified to accommodate the LBHB from the 1-NOH proton and the normal hydrogen bond from the 1-NH proton (Figure 7B).

(iii) A resonance hybrid form of PGH is shown with partial N1═C2 and C2═O2 double bond character (Figure 7B) on the basis of the downfield ^{15}N shift of PGH, $\Delta\delta(^{15}N) = 6$ ppm (Figure 2).

(iv) His-95 Nδ is probably not the recipient of a hydrogen bond from the main chain NH group of Glu-97 as evidenced by the upfield chemical shift value of $\delta(^{15}N) = 121$ ppm (*11*) compared to typical chemical shift values expected for a β-type (—N═) nitrogen not involved in a hydrogen bond (128 ppm) and a hydrogen-bonded β-type nitrogen (138 ppm) (*50*). The probable reason is that the side chain of His-95 is free to rotate between the two orientations shown in Figure 7A and 7B on the basis of NOE's comparable in intensity to the 1-NOH proton resonance of enzyme-bound PGH from both the His-95 CϵH ($\delta = 7.54$ ppm) and the His-95 CδH ($\delta = 6.76$ ppm) in the SS-NOESY experiment (Figure 3).

Alternative Mechanism for the Reaction Catalyzed by TIM. The subtle but important NMR modifications of the X-ray structure of the TIM−PGH complex (Figure 7) suggest an unusually strong hydrogen bond between the carboxyl group of Glu-165 and the O1 oxygen of the enzyme-bound intermediate and a normal hydrogen bond between His-95 NϵH and the C2 oxygen of the intermediate. These observations suggest that the general base, Glu-165, may be involved in proton transfer not only between the C1 and C2 carbons, but also between the O1 and O2 oxygens as in Scheme 3. This mechanism, which has been modified from one proposed for the H95Q mutant of TIM (*51*) by the addition of a LBHB between Glu-165 and O1 of the intermediate, may apply to both wild type and mutant TIM. The NMR relaxation data also provide the exchange rates of the protons in the hydrogen bonds (Figure 5, Table 1).

The first step in the mechanism of Scheme 3 is abstraction of the *pro-R* proton from C1 of DHAP by Glu-165. The proton abstracted from C1 of DHAP is transferred to the O2 oxygen. Subsequently, the proton from O1 of the enediol intermediate is transferred by the second carboxyl oxygen of Glu-165 to C2 to form GAP. This "criss-cross" pattern of proton transfers would be accomodated by (i) the bidentate nature of the carboxyl group and (ii) the presence of two methylene groups in the glutamate side chain enabling rotations about the side chain torsion angles χ_1 and χ_3. The putative role of His-95 in stabilizing the enediol(ate) intermediate(s) and in facilitating proton transfer between the O1 and O2 oxygens has been the subject of considerable study and discussion (*1*, *4*, *6*, *11*, *25*). By donating a normal hydrogen bond, His-95 is responsible for polarizing the substrate carbonyl groups. The carbonyl group of DHAP,

Scheme 3

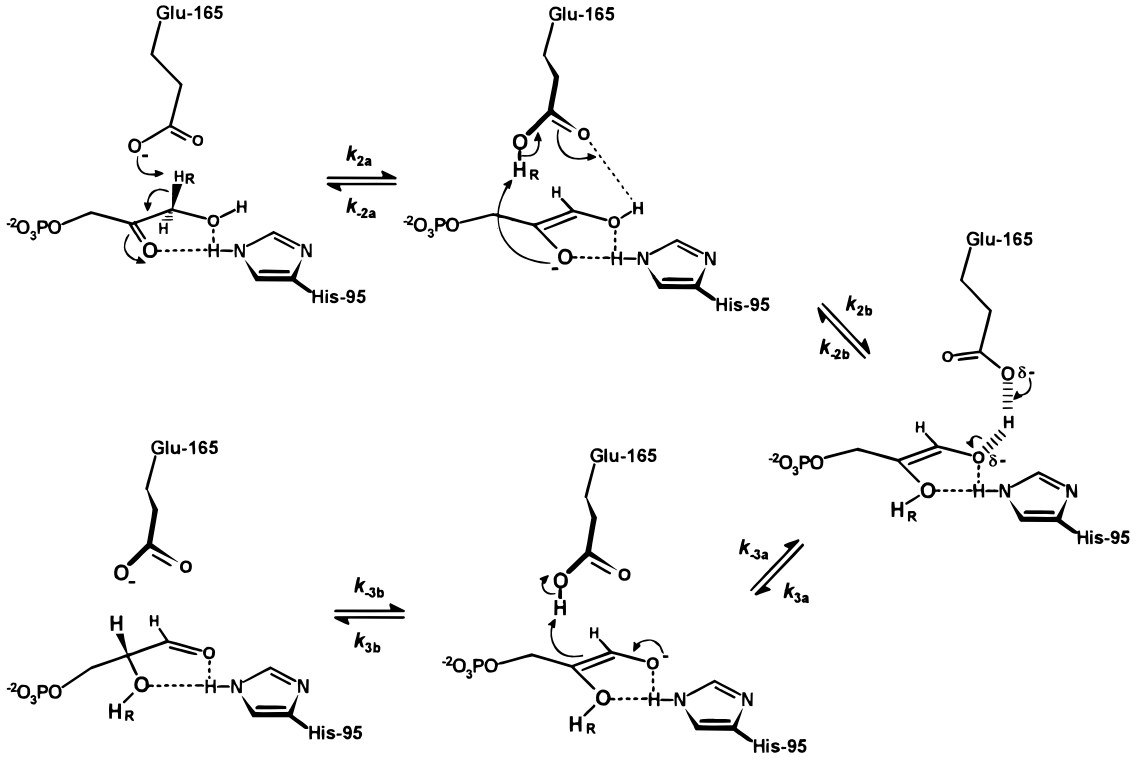

Table 2: Calculation of Proton Exchange Rates (k_{ex}) for an Intramolecular (Scheme 1) or Intermolecular (Scheme 3) Mechanism of Tritium Transfer from DHAP (s/s_o) to GAP (p/s_o) on Triosephosphate Isomerase at 30 °C

				intramolecular (s^{-1})		intermolecular (s^{-1})	
enzyme	k_{cat} (s^{-1})	s/s_o fraction	p/s_o (%)$_{obsd}$	k_{ex}^{calc}	k_{ex}^{obsd}	k_{ex}^{calc}	k_{ex}^{obsd}
yeast TIM (WT)[a]	750	2.0	3.2	1.3×10^5	3.9×10^3	7.5×10^2	80
yeast TIM (H95Q)[b]	5.8	1.2−2.4	<1.0				
chicken TIM (WT)[c]	430	1.3−2.7	2.9−4.4	3.4×10^4	$(3.9 \times 10^3)^e$	103	$(80)^e$
chicken TIM (E165D)[d]	1.8	1.4	2.1	4.6×10^2	$(3.9 \times 10^3)^e$	80	$(80)^e$

[a] From ref (*1*). [b] From ref (*51*). [c] From ref (*37*). [d] From ref (*36*). [e] This value was assumed on the basis of the measured rate on yeast wild type TIM.

which has an infrared absorbance of 1730 cm^{-1} in solution, is shifted to lower wavenumbers when DHAP is bound at the active site (*52*), and no such shift in the DHAP carbonyl stretching frequency was observed on the H95N mutant (*25*). These observations and the relatively modest 140-fold decrease in k_{cat} of the H95Q mutant suggest an essential but limited role for His-95 in catalysis. The stabilization of the enediol intermediate provided by the formation of a LBHB to Glu-165 would further lower the activation free energy of the catalytic steps by a "differential binding" effect (*3*). In contrast, rate enhancement is not attributed to LBHB formation or to full protonation of the substrate carbonyl group by His-95 and thereby lowering of the intrinsic kinetic barrier (*4*, *5*).

Mechanism of Proton Exchange. The fact that the pathway of the reaction catalyzed by TIM involves an intermediate that can exchange protons with solvent has permitted two important kinds of tritium "exchange−conversion" experiments (*53*). First, the fate of the *pro-R* proton in DHAP can be followed by running the reaction of DHAP, specifically labeled with tritium at the *pro-R* position, in unlabeled water. Second, the appearance of tritium in the product and in the remaining substrate can be followed by running the reaction of either unlabeled DHAP or GAP in tritiated water. Kinetic analysis of these reactions has provided details about the rate constants for the individual steps and thereby the Gibbs free energies of the intermediates and transition states for the reaction catalyzed by wild type chicken muscle TIM (*37*), the E165D mutant chicken muscle TIM (*36*), wild type yeast TIM (*1*), and the H95Q mutant of yeast TIM (*51*).

Exchange−conversion experiments showed that wild type and the E165D mutant of TIM catalyzed the transfer of a small amount of tritium label at C1 of DHAP to C2 of the product, GAP (Table 2), and catalyzed progressively increasing amounts of tritium from solvent back into substrate in both the DHAP and GAP directions (*1*, *36*, *37*). In contrast, the H95Q mutant, with only a 140-fold loss in catalytic activity, showed little transfer of tritium either from C1 of DHAP to C2 of GAP or from solvent back into either substrate (*51*). These observations were rationalized by a mechanism for the wild type and E165D enzymes in which Glu-165 catalyzes *intramolecular* proton transfer between the C1 and C2 carbons and His-95 catalyzes proton transfer between the O1 and O2 oxygens (Scheme 1). Exchange with solvent is presumed to occur by reversible proton dissociation from Glu-165 at the intermediate state prior to proton transfer to carbon to form product.

Using Scheme 1, together with all of the reported binding and catalytic rate constants for both protium and tritium

Table 3: Properties of Low-Barrier Hydrogen Bonds on Enzymes As Studied by NMR

enzyme complex	δ (ppm)	assignment	interaction	$\Delta\delta$ (ppm)	ϕ	H-bond strength (kcal/mol)	protection factor
TIM−PGH	14.9	PGH-NOH	E165···HON	6.5	0.38	−	1.0
KSI−DHE[a]	18.2	D99-COOH	D99···Y14	6.2	0.34	≥7.1 (diad)	≥25.5
chymotrypsinogen[b]	18.1	H57-NδH	H57···D102	4.7	0.4	−	9.2
chymotrypsin[c]	18.9	H57-NδH	H57···D102	5.5	−	≥7	−
Asp-amino transferase[d]	17.4	Pyr-NH$^+$	Pyr-NH$^+$···D222	−	−	≥7.6	−
AKB-CoA-ligase[e]	19.1	Pyr-NH$^+$	Pyr-NH$^+$···COO$^-$	−	−	≥3.5	−

[a] From ref (*20*). [b] From ref (*19*). [c] From ref (*18*). [d] From ref (*55*). [e] From ref (*56*).

transfer involved in the interconversion of DHAP and GAP, we have used the program KINSIM (*35*) to calculate the required exchange rate constant (k_{ex}) of Glu-165 with solvent in the enzyme−intermediate complex that yields the observed extent of tritium transfer from DHAP to GAP in wild type and mutant TIM (Table 2). Marked variation of the required k_{ex} is seen, most notably, a 74-fold decrease in the E165D mutant, although the chemical basis for such variation is not clear. Moreover, the required exchange rate for wild type yeast TIM (1.3×10^5 s^{-1}) differs by a factor of 33 from the measured exchange rate of the proton between Glu-165 and the 1-OH in the corresponding TIM−PGH complex (3.9×10^3 s^{-1}). The conclusions from this kinetic analysis also apply to the alternative mechanism involving direct proton transfer from O1 to O2 (*6*).

Another difficulty with a mechanism involving direct proton exchange with solvent from Glu-165 has been pointed out by Rose et al. (*54*) who noted that the loss of such a proton to solvent from the intermediate state, in an intramolecular process, imposes limits on the overall catalytic rate depending on the pK_a of the catalytic base and the pH of the medium. Rose et al. proposed an alternative mechanism for wild type TIM in which the enzyme itself, not the medium, provides a pool of protons with which the enzyme−enediol(ate) intermediate can exchange (*internal exchange*). Exchange of this enzymic pool with the medium (*external exchange*) was proposed to occur after the substrate or product had dissociated. The evidence supporting internal exchange is that tritium, which is exchanged into TIM by incubating in [^{3}H]H$_2$O, is found in the GAP product after the enzyme is diluted into a large volume of unlabeled water containing substrate, DHAP. The observation that exchangeable protons on the enzyme can be fixed into C2 of the product GAP (*54*) together with the finding that the H95Q mutant shows negligible back-exchange of tritium from solvent to substrate or from substrate DHAP to product GAP (*51*) makes it likely that His-95 is a necessary component of the internal exchange process in the wild type enzyme. The assumption by Rose et al. (*54*) that external exchange with the medium occurs only from the free enzyme, however, is inconsistent with the sizable solvent exchange rate which we observe for His-95 NϵH (80 s^{-1}) in the TIM−PGH complex (Figure 5, Tables 1 and 2). Hence, an alternative mechanism to that of Scheme 1 is necessary to explain how the enzyme−intermediate complex avoids the inefficient loss of the abstracted proton at moderate to high pH yet readily exchanges protons with bulk solvent.

Such an alternative mechanism was originally proposed for the H95Q mutant in which Glu-165 carries out all proton transfer steps as in Scheme 3 (*51*). In this mechanism, Glu-165 transfers the *pro-R* proton from the C1 position of DHAP to the O2 enediolate oxygen, a solvent-exchangeable position, so that no transfer of tritium from labeled substrate to product

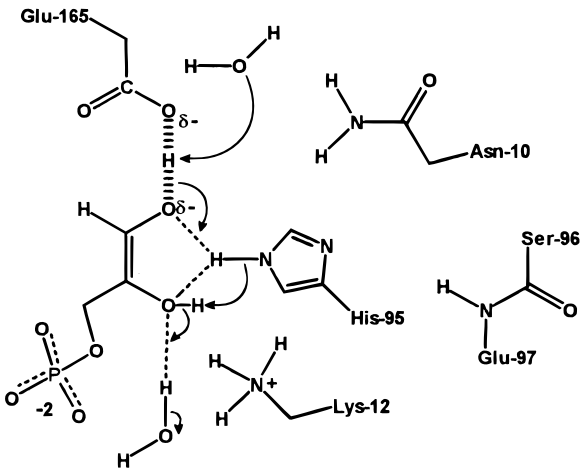

FIGURE 8: Proposed mechanism of exchange of protons at the active site with solvent in the LBHB-stabilized enediol intermediate.

is detectable in the H95Q mutant (Table 2). This mechanism also requires that the carboxyl group of Glu-165 which is transiently protonated with the abstracted *pro-R* proton *does not* exchange its proton with solvent en route to the O2 oxygen to account for the negligible transfer of tritium from solvent back into substrate. The extension of the mechanism of Scheme 3 to the wild type enzyme requires *intermolecular* transfer of tritium label from substrate (DHAP) to product (GAP). The proton exchange mechanism in the LBHB-stabilized intermediate, based on Scheme 3, is shown in Figure 8. In wild type TIM, a fraction of the *pro-R* tritium label is exchanged into the His-95 Nϵ position from O2 in the LBHB-stabilized intermediate (internal exchange). The label may then exchange from His-95 into O1 (internal exchange) and be transferred to GAP in subsequent turnovers. The label may also wash out into solvent from free enzyme or from the enzyme−intermediate complex (external exchange).

Using the binding and catalytic rate constants for both protium and tritium transfer involved in the interconversion of DHAP and GAP as for Scheme 1, we have used KINSIM (*35*) to calculate the required internal exchange rate constants of the proton transferring group in wild type and mutant TIM for the mechanisms of Scheme 3 and Figure 8.[5] These calculated rate constants (Table 2) show reasonable agreement with the measured exchange rate of His-95 NϵH with solvent in the TIM−PGH complex (80 s^{-1}), with the exception of wild type yeast TIM which requires a 9.4 fold faster internal exchange rate due to its higher k_{cat}. Thus, Scheme 3 and Figure 8 provide a better fit to the exchange

[5] The steps described by k_{2a} and k_{2b} in Scheme 3 were described by the single reported rate constant for the chemical step described by k_2 in Scheme 1. The same simplification was made for the pairs of steps described by k_{-2a} and k_{-2b}, k_{3a} and k_{3b}, and k_{-3a} and k_{-3b}.

data than does Scheme 1. The much faster exchange measured for the proton involved in the LBHB between Glu-165 and the NOH proton of bound PGH (3900 s^{-1}) likely reflects the rate of dissociation of PGH from the enzyme, as indicated by its lower activation energy of 8.9 kcal/mol and by the similar exchange behavior of the PGH NH proton resonance, and is therefore irrelevant to the internal exchange process.[4] The 50-fold slower exchange of the His-95 NϵH would permit this residue to function as the carrier for *intermolecular* tritium transfer from substrate to product.

In principle, the ultimate choice between Scheme 1 and Scheme 3 for wild type TIM can be made by further experiments. Intermolecular tritium transfer from DHAP to GAP should show a substrate concentration dependence, while intramolecular transfer should be independent of substrate concentration. A more direct test would be provided by transient-state kinetic studies of tritium transfer in both single and multiple turnovers.

LBHBs on Enzymes. Finally, we note that the strong hydrogen bond between Glu-165 and PGH on TIM is typical of LBHB's found on other enzymes, all of which appear to involve carboxyl groups (Table 3). Thus, deshielded proton resonances at 15−20 ppm, assigned to strong hydrogen bonds have been found at the active sites of Δ^5-3-ketosteroid isomerase between Asp-99 and Tyr-14 (*21*); on chymotrypsin (*18*) and chymotrypsinogen (*19*) between Asp-102 and His-57; on aspartate amino transferase between Asp-222 and the pyridoxal NH^+ (*55*); and on 2-amino-3-ketobutyrate-CoA ligase between a carboxyl group and the pyridoxal NH^+ (*56*). We conclude that Asp and Glu residues on enzymes can play a unique role in catalysis by forming unusually strong hydrogen bonds.

ACKNOWLEDGMENT

We are grateful to Kim Collins for a generous sample of PGH and for helpful discussions, to Elizabeth A. Komives for providing us with expression systems for the H95N mutant of yeast TIM and for helpful advice, and to George H. Reed, Patricia Li Wang, Jeremy R. Knowles, and Irwin A. Rose for valuable comments.

REFERENCES

1. Nickbarg, E. B., and Knowles, J. R. (1988) *Biochemistry 27*, 5939−5947.
2. Albery, W. J., and Knowles, J. R. (1976) *Biochemistry 15*, 5631−5640.
3. Albery, W. J., and Knowles, J. R. (1977) *Angew. Chem., Int. Ed. Engl. 16*, 285−293.
4. Gerlt, J. A., and Gassman, P. G. (1993) *Biochemistry 32*, 11943−11952.
5. Cleland, W. W., and Kreevoy, M. M. (1994) *Science 264*, 1887−1890.
6. Algona, G., Ghio, C., and Kollman, P. A. (1995) *J. Am. Chem. Soc. 117*, 9855−9862.
7. Collins, K. D. (1974) *J. Biol. Chem. 249*, 136−142.
8. Wolfenden, R. (1969) *Nature 223*, 704−705.
9. Zhao, Q., Mildvan, A. S., and Talalay, P. (1995) *Biochemistry 34*, 426−434.
10. Davenport, R. C., Bash, P. A., Seaton, B. A., Karplus, M., Petsko, G. A., and Ringe, D. (1991) *Biochemistry 30*, 5821−5826.
11. Lodi, P. J., and Knowles, J. R. (1991) *Biochemistry 30*, 6948−6956.
12. Kresge, A. J. (1991) *Pure Appl. Chem. 63*, 213−221.
13. Usher, K. C., Remington, S. J., Martin, D. P., and Drueckhammer, D. G. (1994) *Biochemistry 33*, 7753−7759.
14. Kim, H., and Lipscomb, W. N. (1990) *Biochemistry 29*, 5546−5555.
15. Kim, H., and Lipscomb, W. N. (1990) *Biochemistry 30*, 8171−8180.
16. Schowen, K. B., and Schowen, R. L. (1982) *Methods Enzymol. 87*, 551−606.
17. Frey, P. A., Whitt, S. A., and Tobin, J. B. (1994) *Science 264*, 1927−1930.
18. Cassidy, C. S., Lin, J., and Frey, P. A. (1997) *Biochemistry 36*, 4576−4584.
19. Markley, J. L., and Westler, W. M. (1996) *Biochemistry 35*, 11092−11097.
20. Zhao, Q., Abeygunawardana, C., Talalay, P., and Mildvan, A. S. (1996) *Proc. Natl. Acad. Sci. U.S.A. 93*, 8220−8224.
21. Zhao, Q., Abeygunawardana, C., Gittis, A. G., and Mildvan, A. S. (1997) *Biochemistry 36*, 14616−14626.
22. Abeygunawardana, C., Zhao, Q., Talalay, P., and Mildvan, A. S. (1997) *Abstr. Int. Congress Biochem. Mol. Biol., 17th, 1997*, Abstr. No. 177.
23. Harris, T. K., Abeygunawardana, C., and Mildvan, A. S. (1997) *Biophys. J. 72*, A414.
24. Laemmli, U. K. (1970) *Nature 227*, 680−685.
25. Komives, E. A., Chang, L. C., Lolis, E., Tilton, R. F., Petsko, G. A., and Knowles, J. R. (1991) *Biochemistry 30*, 3011−3019.
26. Anderson, V. E., Weiss, P. M., and Cleland, W. W. (1984) *Biochemistry 23*, 2779−2786.
27. Turner, D. L. (1983) *J. Magn. Reson. 54*, 146−148.
28. Marion, D., Ikura, M., Tschudin, R., and Bax, A. (1989) *J. Magn. Reson. 85*, 393−399.
29. Levy, G. C., and Lichter, R. L. (1979) in *Nitrogen-15 Nuclear Magnetic Resonance Spectroscopy*, John Wiley & Sons, New York.
30. Mori, S., Abeygunawardana, C., Johnson, M. O., and van Zijl, P. C. M. (1995) *J. Magn. Reson. 108B*, 94−98.
31. Weber, D. J., Abeygunawardana, C., Bessman, M. J., and Mildvan, A. S. (1993) *Biochemistry 32*, 13081−13088.
32. Smallcomb, S. H. (1993) *J. Am. Chem. Soc. 115*, 4776−4785.
33. Swift, T. J., and Connick, R. E. (1963) *J. Chem. Phys. 37*, 307−320.
34. Anderson, K. S., Sikorski, J. A., and Johnson, K. A. (1988) *Biochemistry 27*, 7395−7406.
35. Barshop, B. A., Wrenn, R. F., and Freiden, C. (1983) *Anal. Biochem. 130*, 134−145.
36. Raines, R. T., Sutton, E. L., Straus, D. R., Gilbert, W., and Knowles, J. R. (1986) *Biochemistry 25*, 7142−7154.
37. Albery, W. J., and Knowles, J. R. (1976) *Biochemistry 15*, 5627−5631.
38. Swain, C. G., Stivers, E. C., Reuwer, J. F., and Schaad, L. J. (1958) *J. Am. Chem. Soc. 80*, 5885.
39. Loh, S. N., and Markley, J. L. (1993) in *Techniques in Protein Chemistry* (Angeletti, R., Ed.) Vol. 4, p 517, Academic Press, San Diego, CA.
40. Lodi, P. J. (1992) *Diss. Abstr. Int. 53-05B*, 90−119.
41. Bax, A., Ikura, M., Kay, L. E., Torchia, D. A., and Tschudin, R. (1990) *J. Magn. Reson. 86*, 304−318.
42. Norwood, T. J., Boyd, J., Heitage, J. E. Soffe, N., and Campbell, I. D. (1990) *J. Magn. Reson, 87*, 488−501.
43. Steinberg, G. M., and Swigler, R. (1955) *J. Org. Chem. 30*, 2362−2365.
44. Bovey, F. A., Jelinski, L., and Mirau, P. A. (1988) in *Nuclear Magnetic Resonance Spectroscopy*, p 94, Academic Press, Inc., New York.
45. Eigen, M. (1964) *Angew. Chem., Intl. Ed. Engl. 3*, 1−19.
46. Lolis, E., Alber, T., Davenport, R. C., Rose, D., Hartman, F. C., and Petsko, G. A. (1990) *Biochemistry 29*, 6609−6618.
47. Kreevoy, M. M., and Liang, T. M. (1980) *J. Am. Chem. Soc. 102*, 3315−3322.
48. Lodi, P. J., Chang, L. C., Knowles, J. R., and Komives, E. A. (1994) *Biochemistry 33*, 2809−2814.
49. McDermott, A., and Ridenour, C. F. (1996) in *Encyclopedia of NMR*, pp 3820−3825, John Wiley & Sons, Ltd, Sussex, England.
50. Bachovchin, W. W. (1986) *Biochemistry 25*, 7751−7759.
51. Nickbarg, E. B., Davenport, R. C., Petsko, G. A., and Knowles, J. R. (1988) *Biochemistry 27*, 5948−5960.

52. Belasco, J. G., and Knowles, J. R. (1980) *Biochemistry 19*, 472−477.
53. Albery, W. J., and Knowles, J. R. (1976) *Biochemistry 15*, 5588−5600.
54. Rose, I. A., Fung, W.-J., and Warms, J. V. B. (1990) *Biochemistry 29*, 4312−4317.
55. Mollova, E. T., Metzler, D. E., Kintanar, A., Kagamiyama, H., Hayashi, H., Hirotsu, K., and Miyahara, I. (1997) *Biochemistry 36*, 615−625.
56. Tong, H., and Davis, L. (1995) *Biochemistry 34*, 3362−3367.

BI972039V